

Scientific paper

Nickel(II) Complex with a Flexidentate Ligand Derived from Acetohydrazide: Synthesis, Structural Characterization and Hirshfeld Surface Analysis

Rasoul Vafazadeh,^{1,*} Zahra Mansouri¹ and Anthony C. Willis²

¹ Department of Chemistry, Yazd University, Yazd, Iran.

² Research School of Chemistry, Australian National University, Canberra, ACT 2601, Australia.

* Corresponding author: E-mail: e-mail address: rvafazadeh@yazd.ac.ir

Tel: +98 351 8214778; Fax: +98 351 7250110

Received: 09-02-2019

Abstract

The mononuclear Ni(II) complex $[\text{Ni}(\text{LP})_2(\text{CH}_3\text{OH})_2]\text{Cl}_2$ has been synthesized by reacting 1-(5-hydroxy-3-methyl-5-phenyl-4,5-dihydro-1H-pyrazol-1-yl)ethan-1-one ligand (HL) with $\text{NiCl}_2 \cdot 6\text{H}_2\text{O}$ in methanol solution. In the reaction, the tridentate ligand, HL, was converted *in situ* into 4-hydroxy-4-phenylbut-3-en-2-ylidene)acetohydrazid ligand, (pyrazole, LP). The pyrazole ligand acts as bidentate neutral ligand and the hydroxyl group is left uncoordinated. The structure of the Ni(II) complex has been established by X-ray crystallography. The Ni(II) is six-coordinate and has a distorted octahedral geometry. It is bonded by two nitrogen and by two oxygen atoms of the two pyrazole ligands and two oxygen atoms of methanol molecules. The Hirshfeld surface analysis and the 2D the fingerprint plot are used to analyses all of the intermolecular contacts in the crystal structures. The main intermolecular contacts are H/H and Cl/H interactions.

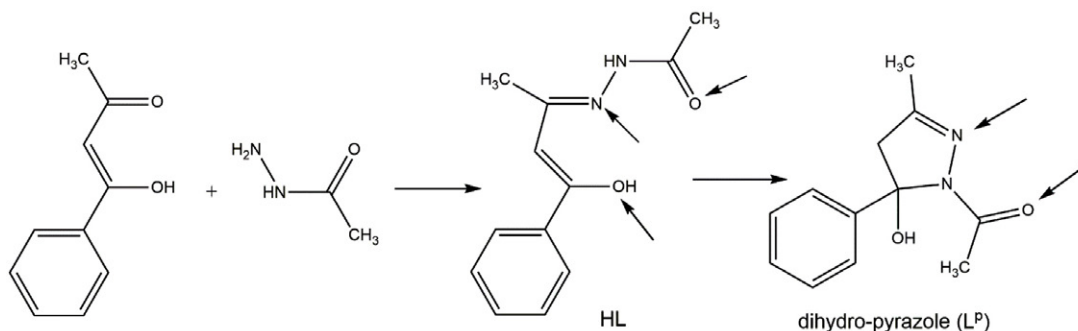
Keyword: Flexidentate ligand; pyrazole ligand; Hirshfeld surface; fingerprint plot; hydroxyl group

1. Introduction

The complexation of transition metal ions with multidentate Schiff base ligands has been studied extensively as their structures can be divers and they can have versatile properties.^{1–3} The hydrazone ligands which are formed by condensation reactions between hydrazide derivatives and relevant aldehyde or ketones, are a signification class of such multidentate ligands. Metal complexes with these ligands can have a wide range of structures with significant

variations in geometry.^{3–7} Also, the cyclization reaction of hydrazide precursors may take place and lead to the formation of pyrazole ligands.^{8–10} The pyrazole compounds themselves are hydrolytically and thermally stable and can act as a mono- or bidentate ligands. The pyrazoles and their complexes can have interesting structural features, properties and biologically actives.^{11–14}

In our previous work, we reported the synthesis of CuLX complexes where HL is 1-(5-hydroxy-3-methyl-5-phenyl-4,5-dihydro-1H-pyrazol-1-yl)ethan-1-one ligand



Scheme 1. Preparation of HL and LP ligands with potential ligating sites

(Scheme 1).¹⁵ In these complexes, the hydrazone ligand was in the keto form and acted as a tridentate monoanionic. In order to investigate the effect of the metal on the coordination behavior of the hydrazone ligand, we report here the reaction of Ni(II) salts with HL. *In situ*, the ligand is converted into the 4-hydroxy-4-phenylbut-3-en-2-ylidene)acetohydrazide ligand, (pyrazole, LP) by the self-cyclization reaction of HL in the presence NiCl₂. The pyrazole coordinates to Ni(II) and act as bidentate neutral ligand and the hydroxyl group is left uncoordinated (Scheme 1).

A search of the literature revealed that the pyrazole had been reported previously by Wang *et al.* and Alberola *et al.* and crystal structure has also been determined.^{16,17} Pyrazole has been prepared by the reaction of 1-phenylbutane-1,3-dione and acetohydrazide in the presence of a catalytic amount of acid under solventless conditions¹⁶ or in solvent.¹⁷

2. Experimental Section

2.1. Starting Materials

All chemicals were of analytical reagent grade and were used without further purification.

Caution! Transition-metal complex perchlorate salts are known to be hazardous and must be treated with care, especially in the presence of organic solvents.

2.2. Physical Measurements

Infrared spectra were taken with an Equinox 55 Bruker FT-IR spectrometer using KBr pellets in the 400–4000 cm⁻¹ range. Absorption spectra were determined using methanol and dimethylformamide (DMF) solutions in a GBC UV-Visible Cintra 101 spectrophotometer with a 1 cm quartz cell, in the range 200–800 nm. Elemental analyses (C, H, N) were performed by using a CHNS-O 2400II PERKIN-ELMER elemental analyzer.

2.3. X-ray Crystallography and Hirshfeld Surfaces Analyses

Single-crystal X-ray diffraction data were collected at 150 K on an Agilent SuperNova diffractometer using Cu K α ($\lambda = 1.54180$ Å) radiation. Data were extracted using the CrysAlis PRO package.¹⁷ The structures were solved by direct methods with the use of SIR92.¹⁹ The structures were refined on F^2 by full matrix least-squares techniques using the CRYSTALS program package.²⁰ The H atoms were initially refined with soft restraints on the bond lengths and angles to regularize their geometry (C–H in the range 0.93–0.98 Å, O–H = 0.83 Å) and with $U_{\text{iso}}(\text{H})$ in the range 1.2–1.5 times U_{eq} of the parent atom. After this, the positions of the H atoms bonded to O and N were refined without constraints whereas those bonded to C ride on the atoms to which they are bonded. Crystallographic data and refinement details for the complex is given in Table 1.

Table 1. Crystallographic data of the complex 1

Compound	[Ni(LP) ₂ (CH ₃ OH) ₂]Cl ₂
Chemical formula	C ₂₆ H ₃₆ Cl ₂ N ₄ NiO ₆
Formula weight	630.21
Temperature (K)	150
Space group	Orthorhombic, <i>Pbca</i> ,
<i>a</i> (Å)	7.3033 (1)
<i>b</i> (Å)	19.2677 (1)
<i>c</i> (Å)	20.4218 (1)
<i>Z</i>	4
<i>F</i> (000)	1320
<i>D</i> _{Calc} (g cm ⁻³)	1.457
Crystal size (mm)	0.22 × 0.12 × 0.11
μ (mm ⁻¹)	3.08
GOF on F^2	1.020
$R[F^2 > 2\sigma(F^2)]$	0.029
$wR(F^2)$ (all data)	0.072*

$$*w = 1/[\sigma^2(F^2) + (0.04P)^2 + 2.1P], \text{ where } P = (\max(F_o^2, 0) + 2F_c^2)/3$$

Hirshfeld surfaces analysis and the associated two-dimensional fingerprint plots for the complexes were calculated with CrystalExplorer 3.1 program.²¹ The d_{norm} surface and 2D fingerprint were used to analyses intermolecular interaction in the crystal packing.

2.4. Syntheses of HL Ligand

The Schiff base ligand, HL, was prepared as previously reported elsewhere by us.¹⁵ Briefly, the ligand was obtained by condensation of equimolar amounts of benzoylacetone (20 mmol, 3.24 g) and acetohydrazide (20 mmol, 1.48 g) in methanol (30 mL). The mixture was refluxed for 2 h during which a light-yellow precipitate was formed. The reaction mixture was then cooled to room temperature and the solid compound formed was filtered. The compound was recrystallized from warm acetone. Yield 67%. IR (KBr, cm⁻¹): $\nu_{\text{C=N}} = 1610$, $\nu_{\text{C=O}} = 1650$. Electronic spectra in acetone: $\lambda_{\text{max}}(\text{nm})$, ($\log \epsilon$): 333 (2.66), 232 (4.29).

2.5. Synthesis of Ni(II) Complex, [Ni(LP)₂(CH₃OH)₂]Cl₂, 1.

This complex was obtained as an unexpected product from following reaction: NiCl₂·6H₂O (2 mmol, 0.475 g) was added to a stirred solution of the ligand HL (2 mmol, 0.434 g) in methanol (30 mL) and the resulting solution was stirred at room temperature for 2 h. The solution's color turned green. After two days, blue block-shaped crystals of the [Ni(LP)₂(CH₃OH)₂]Cl₂ complex suitable for X-ray analysis appeared at the bottom of the vessel. They were filtered off and dried in air. Yield: 61% based on HL. Anal. Calc. for C₂₆H₃₆Cl₂N₄NiO₆: C, 49.55; H, 5.76; N, 8.89%. Found: C, 49.47; H, 5.62; N, 8.84%. IR (KBr, $\nu_{\text{max}}/\text{cm}^{-1}$): $\nu_{\text{C=N}} = 1587$, $\nu_{\text{C=O}} = 1605$. UV-Vis, $\lambda_{\text{max}}(\text{methanol})/\text{nm}$: 784 ($\log \epsilon$, 0.93), 371 (3.50) and 207 (4.54).

By comparison, the corresponding reactions of NiX_2 ($\text{X} = \text{NO}_3^-$ and ClO_4^-) with HL were undertaken under the same conditions, but it was found that new Ni(II) complexes were not formed and the sole product isolated from the preparative mixtures were the initial salt, *i.e.* NiX_2 .

3. Results and Discussion

3.1. Synthesis and Characterization of the Complexes

Complex **1** was obtained by the reactions of $\text{NiCl}_2 \cdot 6\text{H}_2\text{O}$ with an equimolar amount of the ligand HL in methanol solution at room temperature. The reaction of NiCl_2 with HL ligand did not lead to formation of the NiL-Cl complex. The ligand instead was converted *in situ* into the pyrazole ligand, L^{P} under the reaction conditions. L^{P} coordinates to the Ni(II) center, acting as a neutral bidentate ligand and leading to an unexpected product, $(\text{Ni}(\text{L}^{\text{P}})_2(\text{CH}_3\text{OH})_2)\text{Cl}_2$. In contrast, the reaction of copper(II) salts with this ligand did not lead to a cyclization reaction, and the copper complexes which were formed have the ligand acting as a monoanionic tridentate species, *i.e.* $[\text{CuLX}]$.¹⁵ The cyclization reactions in the Ni(II) case may occur due to formation of an unstable Ni(II) complex with HL or Ni(II) may have catalyzed the cyclization reaction.

The IR spectrum of the free HL ligand shows bands at 1610 and 1650 cm^{-1} , which is assigned as $\nu\text{C}=\text{N}$ and $\nu\text{C}=\text{O}$, respectively.^{3,22,23} In the IR spectra of complex, these bands were shifted toward lower energy in comparison with the free ligand, which indicates coordination of the imine nitrogen atom and the carbonyl group to the nickel ion.^{23–25} The fairly broad band of medium intensity appearing at around 3400 cm^{-1} corresponds to the intramolecular hydrogen bonding in the free ligand, this band in the complex is observed in around the 3050 cm^{-1} re-

gion, which indicates that the hydroxyl group remains as an uncoordinated OH group.^{26–28}

3.2. Description of Crystal Structure of the Complex 1

The structural fragment of the complex **1** is shown in Fig. 1. The complex crystallizes in orthorhombic space group $Pbca$ and there are four molecules in the unit cell ($Z = 4$). As shown by Fig. 1, the crystallographic asymmetric unit is one-half of the structural fragment and consists of a Ni(II) atom, one L^{P} ligand, a coordinated methanol and a chloride counter anion. The remainder of the cation is generated by a crystallographic inversion symmetry operation centered on the metal.

The Ni(II) is sixcoordinate (N_2O_4 donor atoms) and has a distorted octahedral geometry. The equatorial plane is formed by two nitrogen and two oxygen atoms from two L^{P} ligands coordinates to the metal center. The ligands with Ni(II) atom formed five-membered chelate rings. The two axial positions are occupied by oxygen atoms of the two methanol molecules.

The Ni–N bond length in the complex is 2.067(1) Å. The Ni–O bond length at the axial position (2.061(1) Å) is slightly longer than the corresponding bond in the equatorial plane (2.037(1) Å). The Ni–O and Ni–N bond lengths of the complex are in good agreement with Ni(II) complexes previously reported.^{29–31} The chelating N–Ni–O angle is 79.37(4)°, whereas the non-chelating N–Ni–O angles is 100.63(4)°. The O3–Ni1–O1 and O3–Ni1–N1 angles are 88.20(4)° and 89.47(5)°, respectively. The C4–O1 bond distance of 1.232(3) Å agrees well with the value of C=O bond as already observed in similar compounds.³² This bond length is similar to the carbonyl group bond length in uncoordinated pyrazole (1.241 and 1.229 Å).^{16,17} The C3–O2 bond length of the alcohol group (1.391(2) Å) is longer than the bond length of the carbonyl group (C4–O1) and similar to C–O(hydroxyl) bond length in uncoor-

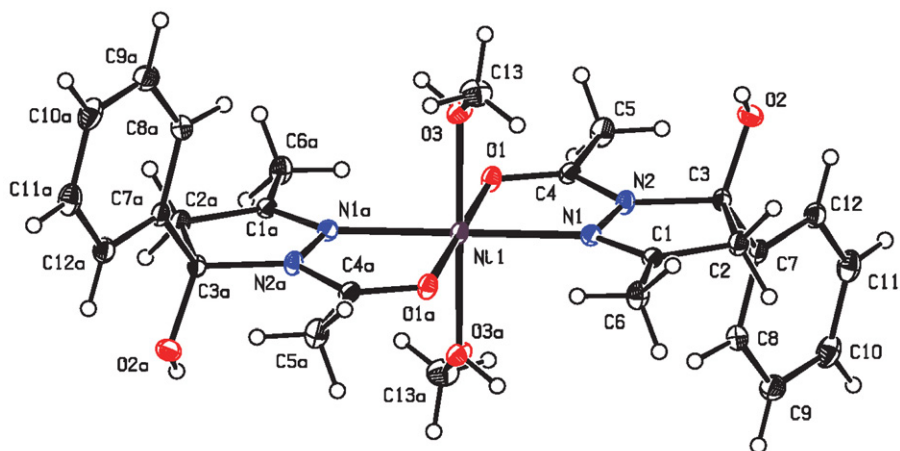


Fig. 1. The molecular structure of complex **1** with labelling of selected atoms, ellipsoids show 30% probability levels (symmetry code: (a) $-x + 1, -y + 1, -z + 1$).

minated pyrazole (1.413 and 1.395 Å).^{16,17} Selected bond lengths and angles, are summarized in Table 2.

The sum of the internal angles of the pyrazole ring in complex **1** [N1–N2–C1–C2–C3 = 539.78°] shows the planarity of this ring since it is very close to the ideal value of 540°. The value is also close to the internal angles of the uncoordinated pyrazole ring uncoordinated (549.78 and 539.61°). The planarity is also illustrated by the small deviations of the atoms of the pyrazole ring from the corresponding mean plane (0.008–0.028 Å). In the uncoordinated pyrazole which was synthesized by Wang et al. and Alberola et al., the deviate from the plane are in the 0.006–0.028 Å and 0.009–0.032 Å rang, respectively.^{16,17}

Table 2. Selected bond lengths (Å) and angles (°) in the Ni(II) complex

Ni1–O1	2.0372(10)	O1–Ni1–N1	79.37(4)
Ni1–O3	2.0606(11)	O1–Ni1–O3	88.20(4)
Ni1–N1	2.0674(12)	O1–Ni1–N1 ^a	100.63(4)
C4–O1	1.2476(18)	N1–Ni1–O3	89.47(5)
C3–O2	1.3914(18)	C3–N2–N1	112.21(10)
C4–N2	1.3434(18)	N2–N1–C1	109.12(11)
C3–N2	1.5160(17)	O1–C4–N2	120.44(13)
C1–N1	1.2814(18)	C3–O2–H2	107.90(17)

Symmetry code: (a) $-x + 1, -y + 1, -z + 1$.

The mean planes of the pyrazole and aromatic rings in complex **1** are almost perpendicular. The dihedral angle is ca. 87.66° which is similar to the values found in uncoordinated pyrazole previously reported (85.73 and 85.79°).^{16,17}

The chloride counter anions are involved in intermolecular and intramolecular hydrogen bonding interaction with the OH groups of the uncoordinated hydroxyl of the ligand and coordinated methanol molecule, which build a

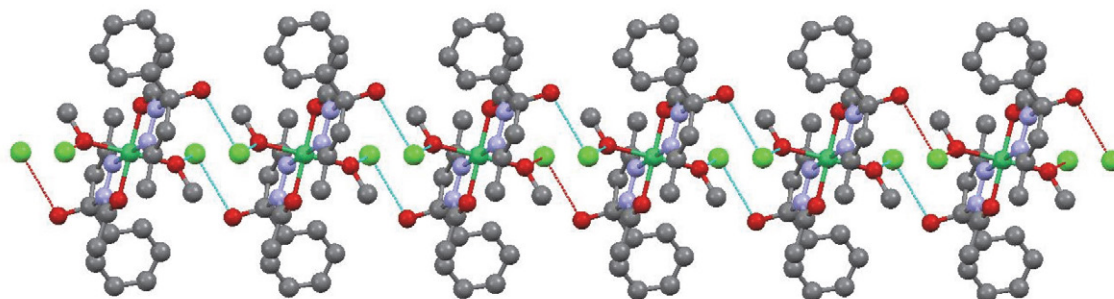


Fig. 2. The hydrogen bonding interactions between uncoordinated hydroxyl group of ligand and the chloride counter anions in complex **1** along *b* axis.

Table 3. Hydrogen bonding (Å) and angles (°) in complex **1**

D–H...A	D–H	H...A	D...A	D–H...A	Symmetry code
O2–H2...Cl1	0.77(2)	2.33(2)	3.093(1)	174.9(19)	$-x, -y + 1, -z + 1$
O3–H3...Cl1	0.83(2)	2.16(2)	2.987(1)	173.0(20)	

1D chain structure running through the *a* axis (Fig. 2). The Ni...Ni distance is 7.303 Å, which is much longer than the van der Waals radii sum for nickel (3.26 Å), showing that there is no interaction between the nickel atoms. The distance between Cl and the center of aromatic ring from adjacent complex and centers of aromatic rings are 6.489 and 7.303 Å, showing that there are no Cl... π and π ... π interactions in the packing for complex **1**.

Full details of the hydrogen bonding are given in Table 3.

3. 3. Hirshfeld Surface Analyses

The Hirshfeld surface analyses and the fingerprint plots provide some useful quantitative information about the strength and role of the intermolecular contacts, and to estimate their importance in the in the crystal packing stability.^{1,26,33,34} In Fig. 3, the 3D Hirshfeld surface mapped are shown over a d_{norm} (normalized contact distance) range of -0.705 – 1.148 Å. The value of the d_{norm} can be

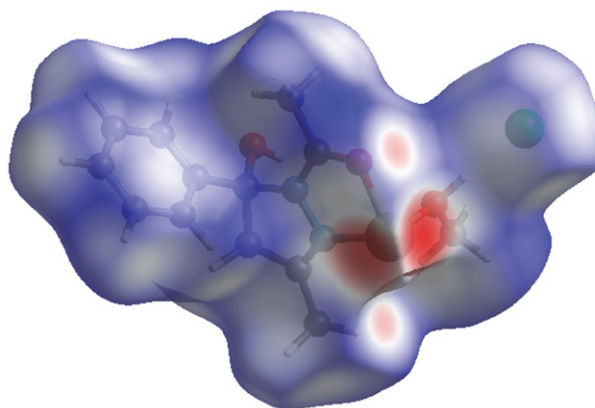


Fig. 3. Hirshfeld surface mapped with d_{norm} for complex **1**.

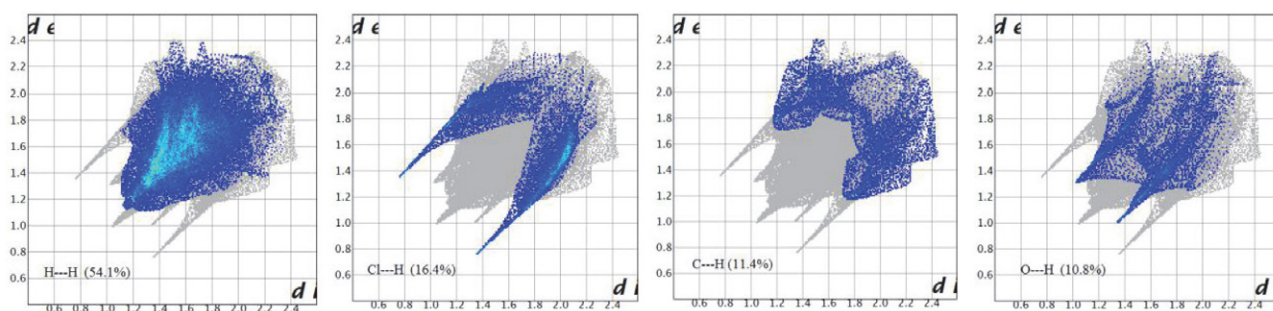


Fig. 4. The 2D fingerprint plots and relative contributions to the percentage of Hirshfeld surface for various interactions in complex 1.

positive or negative when intermolecular contacts are longer or shorter than the sum van der Waals radii of the atoms (vdW), respectively. The d_{norm} values are mapped onto the Hirshfeld surface using a red–blue–white color scheme. Red regions correspond to closer contacts and negative d_{norm} value, the blue regions correspond to longer contacts and positive d_{norm} value. The white-colored regions correspond to weak contacts and the distance of contacts is around the vdW separation ($d_{\text{norm}} \approx 0$).^{33–35}

The 2D fingerprint plot and the contribution of each type of interaction are describe in Fig. 4. The H...H interaction (54.1%) appears as wide and blunt spikes in the region $1.15 \text{ \AA} < (d_e + d_i) < 1.70 \text{ \AA}$. The Cl...H/H...Cl interaction (16.4%) also appears as two distinct spikes, the lower spike corresponding to the acceptor spike represents the Cl...H interactions ($d_i = 1.35 \text{ \AA}$ and $d_e = 0.75 \text{ \AA}$) and the upper spike being a donor spike represents the H...O interactions ($d_e = 1.35 \text{ \AA}$ and $d_i = 0.9 \text{ \AA}$) in the fingerprint plots. Further, the C...H/H...C interaction which comprise 10.2% of the total Hirshfeld surfaces were appeared as two distinct spikes, the C...H interaction with $d_e = 1.17 \text{ \AA}$ and $d_i = 1.70 \text{ \AA}$ and H...C interaction with $d_e = 1.70 \text{ \AA}$ and $d_i = 1.17 \text{ \AA}$. The O...H/H...O interactions comprise 10.8% of the total Hirshfeld surfaces with $d_e = 1.17 \text{ \AA}$ and $d_i = 1.70 \text{ \AA}$ and $d_e = 1.70 \text{ \AA}$ and $d_i = 1.17 \text{ \AA}$ for O...H and H...O interactions, respectively.

4. Conclusion

The $\text{Ni}(\text{LP})_2(\text{CH}_3\text{OH})_2\text{Cl}_2$ complex was obtained as an unexpected product from reaction of NiCl_2 with HL at room temperature. In the Ni(II) complex, metal center is hexacoordinated with a distorted octahedral geometry. The ligand coordinates to the metal center as a neutral bidentate ligand, while in the reaction of copper(II) salts with this ligand, as previously reported, the ligand acts as a monoanionic tridentate ligand. In the reaction with NiCl_2 , the ligand was converted *in situ* into the pyrazole ligand, LP in a cyclization reaction. The Hirshfeld surface analyses and the fingerprint plots provide some useful quantitative information about the role of intermolecular contacts in the crystal packing.

Supplementary material

The deposition numbers of the studied complex is CCDC 1949210. This data can be obtained free-of-charge via www.ccdc.cam.ac.uk/data_request/cif, by emailing data-request@ccdc.cam.ac.uk, or by contacting The Cambridge Crystallographic Data Centre, 12 Union Road, Cambridge CB2 1EZ, UK; fax +44 1223 336033.

Acknowledgments

The authors are grateful to the Yazd University and the Australian National University for partial support of this work.

5. References

- R. Vafazadeh, M. Ehsani1, A. C. Willis, *J. Iran. Chem. Soc.* **2019**, *16*, 2509–2518. DOI:10.1007/s13738-019-01721-3
- T. Ghosh, S. Pal, *Inorg. Chim. Acta* **2010**, *363*, 3632–3636. DOI:10.1016/j.ica.2010.07.007
- R. Vafazadeh, R. Esteghamat-Panah, A. C. Willis, A. F. Hill, *Polyhedron*, 2012, *48*, 51–57. DOI:10.1016/j.poly.2012.08.057
- R. Vafazadeh, Z. Moghadas, A.C. Willis, *J. Coord. Chem.*, **2015**, *68*, 4255–5271. DOI:10.1080/00958972.2015.1096349
- R. Vafazadeh, N. Abdollahi, A.C. Willis, *Acta Chim. Slov.* **2017**, *64*, 409–414. DOI:10.17344/acsi.2017.3263
- A. Mukhopadhyay, S. Pal, *Polyhedron* **2004**, *23*, 1997–2004. DOI:10.1016/j.poly.2004.05.002
- A. Mukhopadhyay, S. Pal, *Eur. J. Inorg. Chem.* **2009**, 4141–4148. DOI:10.1002/ejic.200900472
- R. Vafazadeh, N. Hasanzade, M. M. Heidari, A. C. Willis, *Acta Chim. Slov.* **2015**, *62*, 122–129. DOI:10.17344/acsi.2014.797
- R. Vafazadeh, A. C. Willis, *Acta Chim. Slov.* **2016**, *63*, 186–192.
- K. Sancak, M. Er, Y. Unver, M. Yildirim, I. Degirmencioglu, *Transit. Met. Chem.* **2007**, *32*, 16–22.
- P. P. Devi, F. A.S. Chipem, C. B. Singh, R. K. Lonibala, *J. Mol. Struct.* **2019**, *1176*, 7–18. DOI:10.1016/j.molstruc.2018.08.070
- G. He, X. Hua, N. Yang, L. Li, J. Xu, L. Yang, Q. Wang, L. Ji, *Bioorg. Chem.* **2019**, *91*, 103176–103178. DOI:10.1016/j.bioorg.2019.103176

13. G. A. Gamov, M. N. Zavalishin, A. Y. Khokhlova, A. V. Gashnikova, V. V. Aleksandriiskii, V. A. Sharnin, *J. Coord. Chem.* **2018**, *71*, 3304–3314. DOI:10.1080/00958972.2018.1512708
14. P. Tyagi, M. Tyagi, S. Agrawal, S. Chandra, H. Ojha, M. Pathak, *Spectrochim. Acta A* **2017**, *171*, 246–257. DOI:10.1016/j.saa.2016.08.008
15. R. Vafazadeh, M. Alinaghi, A. C. Willis, A. Benvidi, *Acta Chim. Slov.*, **2014**, *61*, 121–125.
16. Z.-X. Wang, H.-L. Qin, *Green Chem.* **2004**, *6*, 90–92. DOI:10.1039/b312833d
17. A. Alberola, L. Calvo, A. G. Ortega, M. L. Sidaba, M. C. Saiiudo, S. G. Granda, E. G. Rodriguez, *Heterocycles* **1999**, *51*, 2675–2686. DOI:10.3987/COM-99-8683
18. Z. Otwinowski, W. Minor. *Methods in Enzymology*, edited by C. W. Carter Jr & R. M.W. Sweet, New York: Academic Press, **1997**, 276, pp. 307–326. DOI:10.1016/S0076-6879(97)76066-X
19. A. Altomare, G. Cascarano, G. Giacovazzo, A. Guagliardi, M. C. Burla, G. Polidori, M. Camalli, *J. Appl. Cryst.* **1994**, *27*, 435–436. DOI:10.1107/S0021889894000221
20. P. W. Betteridge, J. R. Carruthers, R. I. Cooper, K. Prout, D. J. Watkin, *J. Appl. Cryst.* **2003**, *36*, 1487–1487. DOI:10.1107/S0021889803021800
21. K. Wolff, D. J. Grimwood, J. J. McKinnon, M. J. Turner, D. Jayatilaka, M. A. Spackman. *CrystalExplorer*, Version 3.0. University of Western Australia, **2012**.
22. K. Nakamoto, *Infrared and Raman Spectra of Inorganic and Coordination Compounds*, fourth ed., Wiley, New York, **1986**.
23. R. Vafazadeh, F. Jafari, M. M. Heidari, A.C. Willis, *J. Coord. Chem.* **2016**, *69*, 1313–1325. DOI:10.1080/00958972.2016.1163547
24. M. Shebl, S. M. E. Khalil, *Monatsh Chem.* **2015**, *146*, 15–33. DOI:10.1007/s00706-014-1302-x
25. R. Vafazadeh, B. Khaledi, A. C. Willis, *Acta Chim. Slov.* **2012**, *59*, 954–958.
26. R. Vafazadeh, A. Kazemi-nasab, A. C. Willis, *Acta Chim. Slov.* **2019**, *66*, 1010–1018. DOI:10.17344/acsi.2019.5333
27. M. Barwiolek, E. Szlyk, A. Berg, A. Wojtczak, T. Muziol, J. Jezierska, *Dalton Trans.*, **2014**, *43*, 9924–9933. DOI:10.1039/C4DT00654B
28. M. Dolai, T. Mistri, A. Panja, M. Ali, *Inorg. Chim. Acta* **2013**, *399*, 95–104. DOI:10.1016/j.ica.2013.01.006
29. R. Vafazadeh, M. Namazian, B. Shahpoori-Arani, A. C. Willis, P. D. Carr, *Acta Chim. Slov.* **2018**, *65*, 372–379. DOI:10.17344/acsi.2017.4096
30. L. Radovanović, J. Rogan, D. Poleti, M. V. Rodić, Z. Jagličić, *Acta Chim. Slov.* **2018**, *65*, 191–198. DOI:10.17344/acsi.2017.3813
31. R. Vafazadeh, A. Gorji, S. Ansari, A. C. Willis, *Acta Chim. Slov.* **2012**, *59*, 897–903.
32. P. M. V. Kumar, P. K. Radhakrishnan, *Inorg. Chim. Acta* **2011**, *375*, 84–92. DOI:10.1016/j.ica.2011.04.034
33. M. A. Spackman, D. Jayatilaka, *CrystEngComm* **2009**, *11*, 19–32. DOI:10.1039/B818330A
34. Y. X. Sun, L. Z. Liu, F. Wang, X. Y. Shang, L. Chen, W. K. Dong, *Crystals* **2018**, *8*, 227–239. DOI:10.3390/cryst8050227
35. N. Khelloul, K. Toubal, N. Benhalima, R. Rahmani, A. Chouaih, A. Djafri, F. Hamzaoui, *Acta Chim. Slov.* **2016**, *63*, 619–626. DOI:10.17344/acsi.2016.2362

Povzetek

Sintetizirali smo enojedrni Ni(II) kompleks $[\text{Ni}(\text{LP})_2(\text{CH}_3\text{OH})_2]\text{Cl}_2$ z reakcijo 1-(5-hidroksi-3-metil-5-fenil-4,5-dihidro-1H-pirazol-1-il)etan-1-ona (HL) z $\text{NiCl}_2 \cdot 6\text{H}_2\text{O}$ v metanolu. Tekom reakcije se je trovezni ligand HL *in situ* pretvoril v 4-hidroksi-4-fenilbut-3-en-2-iliden)acetohidrazidni ligand, (pirazol, LP). Pirazolni ligand je dvovezni nevtralni ligand katerega hidroksilna skupina se ne koordinira. Struktura Ni(II) kompleksa je bila določena z rentgensko kristalografijo. Ni(II) ima popačeno oktaedrično geometrijo. Nanj sta vezana dva dušikova atoma in dva kisikova atoma z dveh pirazolskih ligandov ter dve molekuli metanola. Intermolekularni kontakti v kristalni strukturi so bili študirani z Hirshfeldovo analizo površine in 2D diagrami prstnih odtisov. Glavni intermolekularni kontakti so H/H in Cl/H interakcije.



Except when otherwise noted, articles in this journal are published under the terms and conditions of the Creative Commons Attribution 4.0 International License